

---

# A DECOMPOSITION APPROACH FOR LARGE VIRTUAL NETWORK EMBEDDING

---

**Amal Benhamiche**  
 Orange Research  
 F-92320 Châtillon, France  
 amal.benhamiche@orange.com

**Pierre Fouilhoux**  
 Laboratoire d'Informatique de Paris Nord, LIPN, CNRS  
 Université Sorbonne Paris Nord  
 F-93430 Villetaneuse, France  
 pierre.fouilhoux@lipn.univ-paris13.fr

**Lucas Létocart**  
 Laboratoire d'Informatique de Paris Nord, LIPN, CNRS  
 Université Sorbonne Paris Nord  
 F-93430 Villetaneuse, France  
 lucas.letocart@lipn.univ-paris13.fr

**Nancy Perrot**  
 Orange Research  
 F-92320 Châtillon, France  
 nancy.perrot@orange.com

**Alexis Schneider**  
 Orange Research  
 F-92320 Châtillon, France  
 alexis.schneider@orange.com  
 & Laboratoire d'Informatique de Paris Nord, LIPN, CNRS  
 Université Sorbonne Paris Nord  
 F-93430 Villetaneuse, France  
 alexis.schneider@lipn.univ-paris13.fr

December 22, 2025

## ABSTRACT

Virtual Network Embedding (VNE) is the core combinatorial problem of Network Slicing, a 5G technology which enables telecommunication operators to propose diverse service-dedicated virtual networks, embedded onto a common substrate network. VNE asks for a minimum-cost mapping of a virtual network on a substrate network, encompassing simultaneous node placement and edge routing decisions. On a benchmark of large virtual networks with realistic topologies we compiled, the state-of-the-art heuristics often provide expensive solutions, or even fail to find a solution when resources are sparse. We introduce a new integer linear formulation together with a decomposition scheme based on an automatic partition of the virtual network. This results in a column generation approach whose pricing problems are also VNE problems. This method allows to compute better lower bounds than state-of-the-art methods. Finally, we devise an efficient Price-and-Branch heuristic for large instances.

**Keywords** Virtual Network Embedding · Network Slicing · Mathematical Programming · Decomposition · Column Generation

## 1 Introduction

In the early 2000s, *network virtualization* was proposed to overcome the Internet's growing ossification and to foster innovations in networks [1, 2, 3]. In this concept, the physical network hosts multiple *virtual networks*, each with its own architecture, protocols, and users. A virtual network is a logical topology composed of virtual nodes, representing,

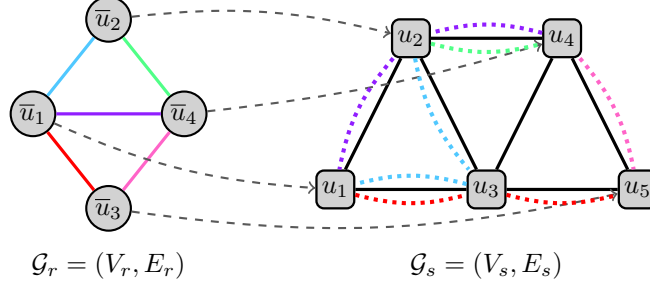


Figure 1: Example of a mapping of a virtual network (on the left) on a substrate network (on the right).

for example, a Virtual Network Function (VNF), a data center or a container, and virtual edges, which imply bandwidth requirements between those nodes. The *infrastructure provider* is responsible for deploying and managing these virtual networks on the underlying physical infrastructure. One of the key challenges in network virtualization is the assignment of virtual elements to the physical infrastructure, which considers simultaneous placement (of the virtual nodes) and routing (of the virtual edges) decisions. The underlying combinatorial problem is known as the Virtual Network Embedding (VNE).

Network virtualization introduces an abstraction layer between service providers and the physical network, enabling flexible, efficient, and automated network management. It was later adopted as a cornerstone of 5G architecture under the name *network slicing* [4, 5]. A *slice* corresponds to an end-to-end virtual network tailored to a specific service or family of services, with specific QoS requirements such as low latency for Ultra-Reliable Low-Latency Communication (URLLC) applications or high bandwidth for Enhanced Mobile Broadband (eMBB). Network slicing is pivotal to enable, within 5G, emerging technologies such as autonomous vehicles or Internet of Things [6, 7, 8]. With the large-scale deployment of 5G Standalone (SA), real-world slices have begun to appear: T-Mobile has introduced a dedicated first-responder slice in the United States [9], while O2 Telefónica and Siemens deployed an industrial slice for the water sector in Germany [10]. These slices cover large portions of the physical network, spanning multiple cities. Because they serve critical services and essential infrastructure (likewise emergency response or water supply), their implementation onto the physical network must be carefully planned to ensure robustness and long-term stability. In this paper, our aim is to propose efficient algorithms for such slice cases.

## 1.1 Problem Statement

The Virtual Network Embedding Problem (VNE) can be defined as follows. We consider simple, connected, undirected graphs. Let us denote the virtual network as  $\mathcal{G}_r = (V_r, E_r)$  with  $n_r$  nodes; and the substrate network as  $\mathcal{G}_s = (V_s, E_s)$  with  $n_s$  nodes. Allocating the substrate resources to the virtual demands is to find a *mapping* (also called an embedding) as follows:

**Definition 1.** A mapping  $m = (m_V, m_E)$  of  $\mathcal{G}_r$  on  $\mathcal{G}_s$  is a pair of functions where:

- $m_V : V_r \rightarrow V_s$  is called the *node placement*;
- $m_E : E_r \rightarrow P_s$ , is called the *edge routing*, where  $P_s$  is the set of loop-free paths of  $\mathcal{G}_s$  and for each  $\bar{e} = (\bar{u}, \bar{v}) \in E_r$ ,  $m_E(\bar{e})$  is a path of  $\mathcal{G}_s$  whose endpoints are  $m_V(\bar{u})$  and  $m_V(\bar{v})$ .

In this work, we consider a *one-to-one* node placement: each virtual node has to be placed on a different substrate node. A substrate node  $u \in V_s$  (resp. a substrate edge  $e \in E_s$ ) has an integer capacity  $c_u$  (resp.  $c_e$ ). Similarly, a virtual node  $\bar{u} \in V_r$  (resp. virtual edge  $\bar{e} \in E_r$ ) has an integer demand  $d_{\bar{u}}$  (resp.  $d_{\bar{e}}$ ). A mapping is said to be *feasible* when the capacity constraints are satisfied, i.e., the sum of the demands of virtual nodes (resp., edges) being placed on a substrate node (resp., being routed on a substrate edge) is less than or equal to the capacity of this node (resp., edge).

Figure 1 illustrates the embedding of a virtual graph on the left over a substrate graph on the right. The dotted arrows show the placement of virtual nodes. A virtual edge of a given color is routed using a substrate path of the same color. In this example,  $m_V(\bar{u}_1) = u_1$ ,  $m_V(\bar{u}_3) = u_5$  and  $m_E(\bar{u}_1, \bar{u}_3) = \{(u_1, u_3), (u_3, u_5)\}$ .

Using a unit of a substrate node (resp. edge) induces a utilization integer cost  $w_u$  (resp.  $w_e$ ). The cost of a mapping  $m$ , denoted  $W_m$ , corresponds to the sum of the placement and routing costs:  $W_m = \sum_{\bar{u} \in V_r} d_{\bar{u}} w_{m_V(\bar{u})} + \sum_{\bar{e} \in E_r} \sum_{e \in m_E(\bar{e})} d_{\bar{e}} w_e$ . The VNE can be formulated as follows:

**Definition 2.** Given a virtual network  $\mathcal{G}_r = (V_r, E_r)$  with demands  $d$ , a substrate network  $\mathcal{G}_s = (V_s, E_s)$  with capacities  $c$  and costs  $w$ , the Virtual Network Embedding Problem (VNE) is to find the minimum cost embedding of  $\mathcal{G}_r$  on  $\mathcal{G}_s$

Introduced after the concept of network virtualization [11, 12], the VNE is recognized as the central combinatorial problem behind resource allocation in network slicing [13].

## 1.2 Related works

The Virtual Network Embedding problem is NP-complete [14, 15], even with uniform demands and topological restrictions [16]. A few special cases are known to be polynomial-time solvable, such as when the virtual network is a uniform-demand star [16, 17]. Several VNE variants have been considered, such as path splitting for virtual edge routing, many-to-one node placement, directed graphs, or location constraints. A survey on many of these variants was conducted in 2013 [18]. We now review the algorithms proposed to solve the VNE problem.

Most of the literature studies VNE in the online context, where small virtual networks arrive over time and must be embedded quickly, to maximize long-term revenue and acceptance rates [19]. In that context, research has mostly focused on heuristics. Early works proposed greedy approaches [11, 20], later refined [21, 22, 23], where first virtual nodes are assigned to substrate nodes based on ranking metrics (e.g., capacities, costs, node centrality, or clustering coefficient), and virtual edges are then routed using shortest-path or multi-commodity flow algorithms. To improve solutions obtained from those greedy heuristics, some authors have considered local search techniques [24, 25] and metaheuristics [26, 27, 28, 29, 30]. Another approach proposed in several works is to decompose the virtual network into smaller subgraphs, and compute mappings for each subgraph and then connect them to obtain a mapping of the whole virtual network [11, 31, 32]. Literature has also considered AI-based methods, with the adaptation of Monte Carlo Tree Search [33], Reinforcement Learning [34, 35] or Graph Neural Network [36, 37] techniques for the VNE problem.

Fewer works have explored mathematical programming approaches. The widely used integer linear formulation for the VNE is the Flow Formulation (FF), based on flow variables and flow conservation constraints [38, 39]. In [19], it is used to devise the rounding heuristic ViNE, extensively used in VNE literature for comparison. The formulation can be easily adapted to additional constraints, such as latency or location constraints [39]. However, it is known to present weak bounds, as discussed in [40, 41]. The Path Formulation (PF) yields tighter bounds by assigning directly virtual edges to substrate paths. Because the set of possible paths grows exponentially, its linear relaxation is commonly solved through Column Generation (CG) [42, 40]. Building on this approach, [42] proposed a Price-and-Branch heuristic, while [40] introduced a full Branch-and-Price algorithm. When embedding multiple virtual networks simultaneously, the Embedding Formulation (EF) has been proposed, where each variable represents the embedding of a whole virtual network. Column generation is used to devise a Price-and-Branch heuristic in [43] and a random rounding heuristic in [44].

## 1.3 Motivation and contributions

Our work is motivated by two limitations in the current VNE literature in the context of Network Slicing. First, VNE has almost exclusively been studied in the online setting, where requests arrive sequentially and must be embedded very quickly. However, many long-term slices, such as those supporting industrial applications or critical infrastructure, must remain in place for long periods of time. Hence, the allocation of resources in the core network should be carefully optimized. This motivates the study of offline VNE on core networks. Second, the recent implementations of country-wide slices [10, 9] indicate that real slices may span large portions of the infrastructure. However, the literature of VNE considers small virtual networks (at most 20 nodes): to the best of our knowledge, only one work has tackled large virtual networks [32]. For such large virtual networks, state-of-the-art heuristics, based on greedy placement strategies, have poor performances and, when capacities are tight, often fail to find any feasible solutions.

We aim to propose algorithms that tackle the embedding of large, realistic virtual networks. To achieve this, we propose a decomposition approach based on a partitioning of the virtual network. The main contributions of this paper are the following:

- We highlight the need for offline VNE in the context of long-term network slices. We introduce large instances based on real core network topologies.
- We introduce the Virtual Partition Formulation, an integer linear formulation based on a tuned partition of the virtual network.
- We solve the linear relaxation of this formulation with a column generation algorithm, to obtain lower bounds.

Virtual Networks				Substrate Networks			
Name	$ V_r $	$ E_r $	Origin	Name	$ V_s $	$ E_s $	Origin
Iris	51	64	TopologyZoo	TataNdl	145	186	TopologyZoo
zib54	54	80	SDN-Lib	GtsCe	149	193	TopologyZoo
HiberniaGlobal	55	81	TopologyZoo	Cogentco	197	243	TopologyZoo
UsSignal	61	77	TopologyZoo				
ta2	65	108	SDN-Lib				
Tw	71	115	TopologyZoo				
Intellifiber	73	95	TopologyZoo				
Uninett2010	74	101	TopologyZoo				
OteGlobe	83	90	TopologyZoo				
Interoute	110	148	TopologyZoo				

Table 1: List of virtual and substrate network instances

- We enhance the pricing scheme to propose an efficient Price-and-Branch heuristic.

The paper is organized as follows. Section 2 introduces a new set of benchmark instances for VNE problems with large virtual networks. Section 3 reviews the classical Flow Formulation and presents our new integer model. Section 4 describes a column generation algorithm used to compute strong lower bounds, which are shown experimentally to outperform those obtained with the Flow Formulation. Section 5 discusses refinements of the pricing scheme that produce columns suitable for constructing high-quality solutions. Based on these developments, we propose a Price-and-Branch heuristic that outperforms state-of-the-art algorithms. Finally, Section 6 concludes the paper.

## 2 Large and realistic instances

Since network virtualization has not yet reached widespread commercial deployment, no practical benchmark of instances exists. This has led previous works to generate random virtual topologies and demands, as well as substrate topologies, capacities, and costs [12, 19, 45, 22, 26, 39]. This over-reliance on randomness makes the instances hard to reproduce and arguably unrealistic. Moreover, the difficulty of an instance, which depends on topologies, demands and capacities, is hard to control. Instead, we propose a new benchmark of reusable and realistic offline VNE instances. These benchmark instances are publicly available at [46] for use in future studies. We consider large virtual networks, since in practice slices may span large portions of the physical networks (e.g. [10, 9]). The generation process, described in detail in [46], is the following.

**Topologies:** In the literature, the standard experimental configuration used relies on small (less than 20 nodes) virtual networks, randomly generated with the GT-ITM tool [47]. Substrate networks (between 100 and 200 nodes) are also generated randomly from GT-ITM. Since the networks generated by GT-ITM are whole networks (core and edge) and not only core ones, we will use instead real large-scale backbone topologies, as resource allocation decisions have the largest impact on long-term investment costs. Those topologies are taken from the Internet Topology Zoo [48] and the Survivable Network Design Library (SNDlib) [49], two widely-used collections in network optimization. These datasets provide Points-of-Presence level representations of backbones from real Internet Infrastructure Providers, at the scale of a country or continent. We selected the largest topologies available in each dataset, which are summarized in Table 1.

**Demands:** Generating realistic demand patterns remains a challenging task, although some attempts have been made in this direction by considering traffic matrices [11, 50]. This leads us to consider, for this study, the simple setting of assigning unit demands to all virtual nodes and edges. This configuration preserves the fundamental simultaneous placement and routing structure of VNE, while removing packing effects that are not central to its difficulty. The insights obtained for this setting remain representative of the general VNE problem. In fact, unit demands can be harder to solve in practice than non-uniform demands, as packing aspects are tackled well by commercial solvers such as CPLEX or Gurobi.

**Capacities and costs:** Substrate nodes and edges capacities are generated randomly, but according to three types: large, medium, and small, as follows. Large capacities are high enough that routing feasibility is never an issue, and any

node placement will induce a solution. These instances allow us to evaluate that algorithms can find good solutions when feasibility is not an issue. For medium capacities, edge capacities are much more restraining, such that edge routing becomes difficult. In small capacities, some substrate nodes (20%) have null capacity, while the edge capacities are even more tight, such that embedding on these substrate networks should be very challenging. Costs are defined following a common principle in real networks: resources with higher capacity and connectivity are cheaper to use, thereby encouraging load balancing. The exact generation of capacities and costs is detailed in [46]. Note that capacities are generated in such a way that every feasible solution for a small-capacity instance is also feasible (with the same cost) in the corresponding medium instance, and likewise for medium vs. large. Hence, the optimal value for small (resp. medium) capacities is always greater than or equal to that of the corresponding medium (resp. large) instance.

### 3 A new formulation based on virtual graph partitioning

In this section, we present the Flow Formulation used for VNE. We discuss the weaknesses of this formulation, leading us to introduce a new formulation based on a partition of the virtual network. In the following, we denote  $v^*$  the optimal value of a given instance. For an integer linear formulation ( $F$ ), its linear relaxation, obtained by relaxing the integrality constraints, is denoted as  $(\tilde{F})$ , and the optimal value of this relaxation as  $v(\tilde{F})$ .

#### 3.1 The (undirected) Flow Formulation

In what follows, we introduce the Flow Formulation for the undirected case. To the best of our knowledge, this formulation has been proposed only for directed graphs [38, 39]. To apply flow conservation constraints, we consider that the edges of  $E_r$  and  $E_s$  are an ordered set, which is equivalent to giving them an arbitrary direction. A virtual edge can traverse a substrate edge  $(u, v) \in E_s$  in both direction  $(u, v)$  or  $(v, u)$ , since the network is undirected. To capture this, we introduce bidirected flow variables: for each substrate edge, we define two variables, one per orientation (original and reverse). This technique is standard in flow problems [51] or network design problems [52].

Two sets of binary variables are considered. The placement variable  $x_{\bar{u}u}$  takes the value 1 if and only if the virtual node  $\bar{u} \in V_r$  is placed on substrate node  $u \in V_s$ . The flow variable  $y_{\bar{e}e_+}$  (resp.  $y_{\bar{e}e_-}$ ) takes the value 1 if and only if the path routing virtual edge  $\bar{e} \in E_r$  uses substrate edge  $(u, v) = e \in E_s$ , from  $u$  to  $v$  (resp. from  $v$  to  $u$ ). For a (directed) edge  $e$ , its start (resp. terminal) node is denoted  $s(e)$  (resp.  $t(e)$ ). For a node  $u \in V_s$ , its adjacent edges are denoted  $\delta(u)$ . Additionally, we denote  $\delta^+(u) = \{e_+ : s(e) = u\} \cup \{e_- : t(e) = u\}$ , which corresponds to the outgoing arcs of the node  $u$  on the bidirected version of the substrate network. The Flow Formulation ( $FF$ ) is the following.

$$\begin{aligned}
\min \quad & \sum_{u \in V_s} \sum_{\bar{u} \in V_r} d_{\bar{u}} w_u x_{\bar{u}u} + \sum_{e \in E_s} \sum_{\bar{e} \in E_r} d_{\bar{e}} w_e (y_{\bar{e}e_+} + y_{\bar{e}e_-}) \\
\text{s.t.} \quad & \sum_{u \in V_s} x_{\bar{u}u} = 1 && \forall \bar{u} \in V_r && (1a) \\
& x_{s(\bar{e})u} - x_{t(\bar{e})u} = \sum_{e \in \delta(u)} y_{\bar{e}e_+} - y_{\bar{e}e_-} && \forall \bar{e} \in E_r, \forall u \in V_s && (1b) \\
& \sum_{\bar{u} \in V_r} x_{\bar{u}u} \leq 1 && \forall u \in V_s && (1c) \\
& \sum_{\bar{u} \in V_r} d_{\bar{u}} x_{\bar{u}u} \leq c_u && \forall u \in V_s && (1d) \\
& \sum_{\bar{e} \in E_r} d_{\bar{e}} (y_{\bar{e}e_+} + y_{\bar{e}e_-}) \leq c_e && \forall e \in E_s && (1e) \\
& \sum_{e: s(e)=u} y_{\bar{e}e} \geq x_{s(\bar{e})u} && \forall \bar{e} \in E_r, \forall u \in V_s && (1f) \\
& x_{\bar{u}u} \in \{0, 1\} && \forall \bar{u} \in V_r, \forall u \in V_s, && \\
& y_{\bar{e}e_+}, y_{\bar{e}e_-} \in \{0, 1\} && \forall \bar{e} \in E_r, \forall e \in E_s &&
\end{aligned}$$

The objective function expresses an embedding cost taking into account placement and routing costs. The constraints (1a) ensure valid virtual nodes placement. The constraints (1b) are the flow conservation constraints and guarantee that each virtual edge is associated with a routing path in the substrate graph whose end nodes host its endpoints. The one-to-one node placement is enforced by constraints (1c). Constraints (1d) (resp. (1e)) ensure that node (resp. edge) capacities are respected. Finally, the Constraints (1f) are the flow departure constraints: they are new valid inequalities

for the VNE in the one-to-one node placement case. They permit to greatly reinforce the linear relaxation. They translate that, when a virtual node is placed on a substrate node, adjacent edges to the virtual node are routed on adjacent edges to this substrate node.

### 3.2 The new Virtual Partition Formulation

Unfortunately, the Flow Formulation suffers from poor linear relaxation [41, 40], which we have observed in our preliminary tests, even with the flow departure constraints. To obtain better lower bounds, the Path Formulation has been proposed [42, 40], where variables indicate whether a virtual edge is routed using a given substrate path. Since there is an exponential number of variables, the linear relaxation is solved by column generation (CG) [53]. However, in our early tests, the Path Formulation only proposed a slightly better linear relaxation than the Flow Formulation reinforced with flow departure constraints, at the cost of longer running times.

Our idea is that, to get a better linear relaxation, a decomposition should consider a larger sub-component than a single virtual edge: a *virtual subgraph* of several connected nodes and edges. This is achieved through a partition of the virtual network into smaller subgraphs, which can be embedded efficiently through existing methods. This idea has practical relevance: it can be expected that the virtual network is composed of cohesive regions, e.g., part of a slice can be dedicated to a specific service or location, which can be tackled with dedicated routines. Solving VNE through a partition of the virtual network into stars [11] or cycles and paths [31] has already been studied in a few heuristics [32, 11, 31]. In this work, we propose a formal framework, based on a new integer linear formulation for VNE: the Virtual Partitioning Formulation.

Given a subset of virtual nodes  $V_r' \subseteq V_r$ , the *induced subgraph* of  $\mathcal{G}_r$  on  $V_r'$  is the graph  $\mathcal{G}_r' = (V_r', E_r')$ , where  $E_r' = \{(u, v) \in E_r : u, v \in V_r'\}$ . In the following, we will often omit the word *induced*. Now consider a partition of the virtual nodes of  $\mathcal{G}_r$  into  $1 \leq k_r \leq n_r$  subsets  $\pi = (V_r^1, \dots, V_r^{k_r})$ , such that  $V_r = \cup_{i \in \{1, \dots, k_r\}} V_r^i$  (every node belongs to exactly one subset) and  $|V_r^i| \geq 1$  for  $i \in \{1, \dots, k_r\}$ . For each part  $V_r^i$ , we denote the corresponding induced subgraph by  $\mathcal{H}_r^i$ . The subgraph containing a node  $\bar{u} \in V_r$  is denoted  $\mathcal{H}_r(\bar{u})$ . Edges that connect nodes in different subsets do not belong to any subgraph  $\mathcal{H}_r^i$ . We denote this set of *cut edges* by  $E_r^0$ . The set of feasible sub-mappings of a subgraph  $\mathcal{H}_r^i$  is denoted  $\mathcal{M}_i$ . The cost of a sub-mapping  $m \in \mathcal{M}_i$  is denoted  $w_m$ .  $x_{\bar{u}u}^m$  is equal to one iff  $\bar{u}$  is placed on  $u$  in  $m$ ,  $y_{\bar{e}e_+}^m$  (resp.  $y_{\bar{e}e_-}^m$ ) is equal to one iff the path routing  $\bar{e}$  uses substrate edge  $(u, v) = e \in E_s$ , from  $u$  to  $v$  (resp. from  $v$  to  $u$ ) in  $m$ .

Two sets of binary variables are considered. The *sub-mapping* variables, denoted  $\lambda_m^i$ , take the value 1 if and only if the mapping  $m \in \mathcal{M}_i$  is selected for subgraph  $\mathcal{H}_r^i$ ,  $i \in \{1, \dots, k_r\}$ . Flow variable  $y_{\bar{e}e_+}$  (resp.  $y_{\bar{e}e_-}$ ) takes the value 1 if and only if the path routing virtual cut edge  $\bar{e} \in E_r^0$  uses substrate edge  $(u, v) = e \in E_s$ , from  $u$  to  $v$  (resp. from  $v$  to  $u$ ). The Virtual Partition Formulation for the partitioning  $\pi$ , denoted  $VPF_{\pi}$ , is the following.

$$\begin{aligned}
\min \quad & \sum_{i \in \{1, \dots, k_r\}} \sum_{m \in \mathcal{M}_i} w_m \lambda_m^i + \sum_{e \in E_s} \sum_{\bar{e} \in E_r^0} w_e d_{\bar{e}} (y_{\bar{e}e_-} + y_{\bar{e}e_+}) \\
\text{s.t.} \quad & \sum_{m \in \mathcal{M}_i} \lambda_m^i \geq 1 & \forall i \in \{1, \dots, k_r\} & (2a) \\
& \sum_{\substack{m \in \mathcal{M}_i, \\ s(\bar{e}) \in V_r^i}} x_{s(\bar{e})u}^m \lambda_m^i - \sum_{\substack{m \in \mathcal{M}_i, \\ t(\bar{e}) \in V_r^i}} x_{t(\bar{e})u}^m \lambda_m^i = \sum_{e \in \delta(u)} y_{\bar{e}e_+} - y_{\bar{e}e_-} & \forall \bar{e} \in E_r^0, \forall u \in V_s & (2b) \\
& \sum_{i \in \{1, \dots, k_r\}} \sum_{m \in \mathcal{M}_i} \sum_{\bar{u} \in V_r^i} x_{\bar{u}u}^m \lambda_m^i \leq 1 & \forall u \in V_s & (2c) \\
& \sum_{i \in \{1, \dots, k_r\}} \sum_{m \in \mathcal{M}_i} \sum_{\bar{u} \in V_r^i} d_{\bar{u}} x_{\bar{u}u}^m \lambda_m^i \leq c_u & \forall u \in V_s & (2d) \\
& \sum_{i \in \{1, \dots, k_r\}} \sum_{m \in \mathcal{M}_i} \sum_{\bar{e} \in E_r^0} d_{\bar{e}} (y_{\bar{e}e_-}^m + y_{\bar{e}e_+}^m) \lambda_m^i + \sum_{\bar{e} \in E_r^0} d_{\bar{e}} (y_{\bar{e}e_+} + y_{\bar{e}e_-}) \leq c_e & \forall e \in E_s & (2e) \\
& \sum_{\substack{m \in \mathcal{M}_i, \\ s(\bar{e}) \in V_r^i}} x_{s(\bar{e})u}^m \lambda_m^i \leq \sum_{e \in \delta^+(u)} y_{\bar{e}e} & \forall \bar{e} \in E_r^0, \forall u \in V_s & (2f) \\
& \lambda_m^i \in \{0, 1\} & \forall m \in \mathcal{M}_i, \forall i \in \{1, \dots, k_r\} \\
& y_{\bar{e}e_+}, y_{\bar{e}e_-} \in \{0, 1\} & \forall \bar{e} \in E_r, \forall e \in E_s
\end{aligned}$$

Constraints (2a) are the convexity constraints of the formulation, ensuring that one mapping is selected for each subgraph. Constraints (2b) (resp. (2d)) are the flow conservation (resp. flow departure) constraints for the virtual cut edges. The one-to-one node placement is enforced by constraints (2c). Inequalities (2e) (resp. (2f)) ensure that substrate node (resp. edge) capacities are respected.

### 3.3 Formulations comparison

This decomposition is quite unusual, as columns have the same structure (a feasible mapping for a virtual network) as the solution for the overall problem. Such a decomposition is similar to what is done in [54], on a Temporal Knapsack problem, where it is coined as a *Recursive Dantzig-Wolfe Decomposition*. Moreover,  $(VPF)$  has a similar structure to  $(FF)$ : the flow conservation and flow departure constraints remain for the virtual cut edges, whereas placement of nodes is replaced by the mapping of a subgraph of the virtual network. If a subgraph corresponds to a single virtual node, then the sub-mapping variable corresponds to a classical placement variable from the flow formulation. In that case,  $(VPF)$  and  $(FF)$  are the same formulation. On the other hand, if  $k_r = 1$ , then the only subgraph is the entire virtual network and  $v(\widetilde{VPF}) = v^*$ . In what follows, we will study a few properties of  $(VPF)$ , using the instance from Example 1 for illustration.

**Example 1.** Figure 2 provides an instance of VNE. The virtual network, on the left, has unit demands on all nodes and edges. The substrate network, on the right, has unit capacities on all nodes and edges, with zero cost on nodes and unit cost on edges. For this instance,  $v(\widetilde{FF}) = |E_r|$ .

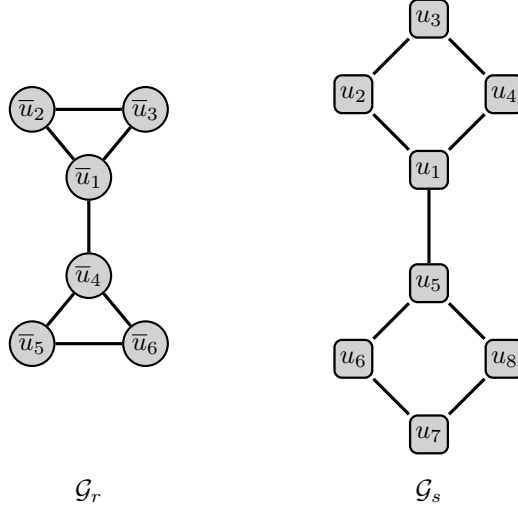


Figure 2: A VNE instance

First, let us show that our new formulation has a better linear relaxation than the Flow Formulation.

**Proposition 1.**  $v(\widetilde{FF}) \leq v(\widetilde{VPF}_\pi)$ , for any partition  $\pi$  of the virtual network, and the gap between the two can be arbitrarily large.

*Proof.* Consider a  $k_r$  partition  $\pi$  of the virtual network. Given a fractional solution  $(\lambda, y)$  to  $(\widetilde{VPF}_\pi)$ , a valid solution  $(x, y')$  to  $(\widetilde{FF})$  can be built as follows:

- For  $i \in \{1, \dots, k_r\}$ , for  $\bar{u} \in V_r^i$ , set  $x_{\bar{u}u} = \sum_{m \in \mathcal{M}_i} x_{\bar{u}u}^m \lambda_m^i$
- For  $i \in \{1, \dots, k_r\}$ , for  $\bar{e} \in E_r^i$ , set  $y_{\bar{e}e_-} = \sum_{m \in \mathcal{M}_i} y_{\bar{e}e_-}^m \lambda_m^i$  and  $y_{\bar{e}e_+} = \sum_{m \in \mathcal{M}_i} y_{\bar{e}e_+}^m \lambda_m^i$
- For  $\bar{e} \in E_r^0$ , set  $y'_{\bar{e}e_-} = y_{\bar{e}e_-}$  and  $y'_{\bar{e}e_+} = y_{\bar{e}e_+}$  for any  $e \in E_s$ .

Thus  $v(\widetilde{FF}) \leq v(\widetilde{VPF}_\pi)$ . Now, consider the instance of Example 1 and the partitioning of the virtual network in the two triangles  $\pi = \{\{\bar{u}_1, \bar{u}_2, \bar{u}_3\}, \{\bar{u}_4, \bar{u}_5, \bar{u}_6\}\}$ . Any sub-mapping of one of the two virtual triangle subgraphs has a cost of 4, since they have to be embedded on one of the substrate squares. Thus  $v(\widetilde{VPF}) = |E_s| > v(\widetilde{FF})$ . By considering larger substrate cycles instead of the two squares, the gap between the two relaxations can be increased to an arbitrarily large value.  $\square$

We will now prove a stronger result. A partition  $\pi'$  is a *refinement* of  $\pi$  if every part of  $\pi'$  is included in some part of  $\pi$ .

**Proposition 2.** *Let  $\pi$  and  $\pi'$  be two partitions of  $V_r$  such that  $\pi'$  is a refinement of  $\pi$ . Then  $v(\widetilde{VPF}_\pi) \geq v(\widetilde{VPF}_{\pi'})$ , and the gap between the two can be arbitrarily large.*

*Proof.* We note  $\pi = \{V_r^1, \dots, V_r^{k_r}\}$  and  $\pi' = \{V_r'^1, \dots, V_r'^{k'_r}\}$ , with  $k_r \geq k'_r$ . For  $i \in \{1, \dots, k'_r\}$ , let  $\phi(i)$  denote the index of the part  $V_r^{\phi(i)}$  containing  $V_r'^i$ . Given a solution  $(\lambda, y)$  to  $(\widetilde{VPF}_\pi)$ , a solution  $(\lambda', y')$  to  $(\widetilde{VPF}_{\pi'})$  of same costs can be built as follows.

- For  $i \in \{1, \dots, k'_r\}$ , for each sub-mapping  $m \in \mathcal{M}_{\phi(i)}$  of  $\mathcal{H}_r^{\phi(i)}$ , a sub-mapping  $m'$  for  $\mathcal{H}^i$  can be constructed by considering the node placement and edge routing of nodes and edges of  $\mathcal{H}^i$  in  $m$ . Set  $\lambda_{m'}^i = \lambda_m^{\phi(i)}$ .
- For  $\bar{e} \in E_r^0$ , simply set  $y'_{\bar{e}e_-} = y_{\bar{e}e_-}$  and  $y'_{\bar{e}e_+} = y_{\bar{e}e_+}$ .

Thus  $v(\widetilde{VPF}_\pi) \geq v(\widetilde{VPF}_{\pi'})$ . Now, consider again the instance of Example 1. With  $\pi = \{\{\bar{u}_1, \bar{u}_2, \bar{u}_3\}, \{\bar{u}_4, \bar{u}_5, \bar{u}_6\}\}$  and  $\pi' = \{\{\bar{u}_1\}, \{\bar{u}_2\}, \{\bar{u}_3\}, \{\bar{u}_4\}, \{\bar{u}_5\}, \{\bar{u}_6\}\}$ ,  $\pi'$  is a refinement of  $\pi$ . As shown earlier  $v(\widetilde{VPF}_\pi) = |E_s| > v(\widetilde{FF}) = v(\widetilde{VPF}_{\pi'}) = |E_r|$ , and the gap can be increased to an arbitrarily large value with larger substrate cycles.  $\square$

This shows that using a smaller  $k_r$  will typically lead to better relaxation values. However, it is not always the case:

**Remark 1.** *Let  $\pi$  and  $\pi'$  be two partitions of  $V_r$  of sizes respectively  $k_r$  and  $k'_r$ , with  $k_r > k'_r$ . In some cases,  $v(\widetilde{VPF}_\pi) > v(\widetilde{VPF}_{\pi'})$ .*

*Proof.* Consider again the instance of Example 1 and the partitions  $\pi = \{\{\bar{u}_1, \bar{u}_2, \bar{u}_3\}, \{\bar{u}_4\}, \{\bar{u}_5\}, \{\bar{u}_6\}\}$  and  $\pi' = \{\{\bar{u}_1, \bar{u}_2\}, \{\bar{u}_3, \bar{u}_4\}, \{\bar{u}_5, \bar{u}_6\}\}$ . Although  $\pi$  has more parts,  $v(\widetilde{VPF}_\pi) > v(\widetilde{VPF}_{\pi'})$ .  $\square$

In this example, a better bound is obtained with a denser (cyclic) subgraph, rather than larger (in average) path subgraphs.

## 4 Column generation and lower bounds

In this section, we describe our column generation implementation to solve the linear relaxation  $(\widetilde{VPF})$  and compute strong lower bounds.

### 4.1 Automatic partition of the virtual network

First, we propose a partitioning strategy. The quality of the virtual network partition is crucial for the efficiency of our algorithm, as suggested by the observations in Section 3.3. We opt for two widely used automatic graph partitioners, KaHIP [55] and METIS [56]. Both algorithms aim to produce balanced partitions while minimizing the number of cut edges, which is particularly desirable in our case. In practice, we found that KaHIP usually yields higher quality partitions, but the subgraphs produced are occasionally disconnected, and correcting the issue can significantly unbalance the partition. In such cases, we resort to METIS, which allows us to enforce connectivity explicitly. For the graph sizes considered in our experiments, both algorithms run extremely fast (below one millisecond).

## 4.2 Column generation for $(\widetilde{VPF})$

Column generation is an algorithm that solves linear programs with an exponential number of variables [53], by adding iteratively its variables, or *columns*. The Restricted Master Problem (*RMP*) refers to  $(VPF)_\pi$  with a subset of columns. A *Pricing Problem* generates the column with the lowest reduced costs. When no columns with negative reduced costs are found,  $(\widetilde{RMP})$  has been solved to optimality. In our case, for a given virtual subgraph  $\mathcal{H}_r^i$ ,  $i \in \{1, \dots, k\}$ , the pricing problem  $PP_i$  is actually a VNE problem of the virtual subgraph  $\mathcal{H}_r^i$  on  $\mathcal{G}_s$ . It can be solved using the Flow Formulation, with the following objective function:

$$\begin{aligned}
v(PP_i) = \min & -\theta_i + \sum_{u \in V_r^i} \sum_{\bar{u} \in V_s} (w_u - \phi_u - \beta_u) x_{\bar{u}u} + \sum_{e \in E_s} \sum_{\bar{e} \in E_r^i} (w_e - \beta_e) y_{\bar{e}e} \\
& + \sum_{\substack{\bar{e} \in E_r^0 \\ t(\bar{e}) \in V_r^i}} \sum_{u \in V_s} \alpha_{\bar{e}u} x_{t(\bar{e})u} - \sum_{\substack{\bar{e} \in E_r^0 \\ s(\bar{e}) \in V_r^i}} \sum_{u \in V_s} \alpha_{\bar{e}u} x_{s(\bar{e})u} \\
& - \sum_{u \in V_s} \sum_{\substack{\bar{e} \in E_r^0 \\ s(\bar{e}) \in \mathcal{H}_r^i}} \gamma_{\bar{e}u} x_{s(\bar{e})u}
\end{aligned} \tag{3}$$

where the dual variables  $\theta, \alpha, \phi, \beta, \gamma$  correspond to respectively inequalities (2a), (2b), (2c), (2d) and (2e), (2f).

Although the convergence of the column generation algorithm can take a long time, the *Lagrangian bound* proposes a valid lower bound for the problem and can be computed easily at each step of the algorithm:

$$LGB = v(\widetilde{RMP}) + \sum_{i \in \{1, \dots, k_r\}} v^*(PP_i) \tag{4}$$

## 4.3 Stabilization

We observed oscillations in the dual variables during our tests, in particular for the dual variables  $\beta$ , related to the flow conservation constraints, which can take both positive and negative values. At a given iteration of the column generation, when dual variables are far from their optimal values, it results in weak columns. This behaviour is a well-known issue in column generation. To mitigate these oscillations, we adopt a standard stabilization technique: dual variable smoothing [57]. At each iteration, instead of using the current dual variables from the restricted master problem, we use a convex combination of the previous stabilized duals and the current ones. The parameter  $\alpha \in [0, 1]$  controls the smoothing strength. At a given iteration of the column generation, the stabilized counterpart  $\hat{\omega}$  of the dual variable  $\omega$  is:

$$\hat{\omega} = \alpha \hat{\omega}' + (1 - \alpha) \omega$$

where  $\hat{\omega}'$  is the stabilized variable at the previous iteration. In practice, we use  $\alpha = 0.9$ , which showed good results in [57]. Preliminary experiments showed that this stabilization improves the performance of the column generation by around 5%, at no computational costs.

## 4.4 Heuristic sub-pricers

Solving the pricing problems optimally can be very time-consuming. The most efficient algorithms to solve the pricing problems optimally are MILP solvers such as IBM ILOG CPLEX (referred to as CPLEX), using the Flow Formulation. However they have long solving times even for quite small virtual networks on a large substrate network: often more than a minute with  $n_r = 10$  and  $n_s = 150$ . Since exact pricers are too expensive, we will only use them at the end of the CG, in order to provide a strong lower bound.

Before, we use heuristic *sub-pricers*, which are pricers restricted to a substrate subgraph. These substrate subgraphs of the sub-pricers are generated as follows. The substrate is partitioned into a large number of parts, using KaHIP or METIS as previously mentioned. Then each substrate subgraph is expanded by adding neighbouring nodes, up to roughly three times the virtual subgraph average size. This method offers three advantages.

- A sub-pricer contains very good columns, if the substrate subgraphs are large enough. Indeed, good sub-mappings will not usually span a large part of the substrate network, as it would induce high routing costs.

- Selecting the size of the subgraph provides a good way to balance column quality and sub-pricer difficulty (and runtime when using an exact solver).
- All constraints of the  $(RMP)$  are covered, which is typically very helpful for convergence of the CG. Indeed, the columns are diverse and pave all parts of the substrate network, since we generated diverse substrate subgraphs.

**Exact sub-pricers** correspond to solving a sub-pricer with an exact solver (CPLEX in our case).

**Greedy sub-pricers** Since solving sub-pricers exactly can still consume too much time and we want to generate quickly many columns at the first iterations, we also propose to use the greedy heuristic described in Algorithm 1 to solve the sub-pricer. This greedy heuristic works as follows. First, the virtual node placement is initialized, with a random virtual node being placed on a random substrate node. Then, virtual nodes are placed one by one. The next virtual node to be placed must have at least one neighbor already placed (the neighbors of a node  $\bar{u}$  are denoted  $N(\bar{u})$ ). Substrate nodes are ranked according to their distance to other substrate nodes hosting neighbors of the virtual node (list  $l$ ). The virtual node is placed on the best substrate node. When all virtual nodes are placed, the virtual edge routing is achieved by solving successive shortest paths problems on residual edge capacities. This greedy heuristic is similar to those of works [21, 22, 23]. However, in these works, the node placement is achieved by ranking substrate nodes based on their capacity, cost, and connectivity. We found that ranking based on the distances was much more effective in our case. When the virtual subgraph is small, the heuristic usually provides a reasonably good mapping, while running very fast (well under 0.01 seconds) because the substrate subgraph is small. Since it is so cheap, we run the heuristic 100 times and keep the mapping with the best reduced cost. Columns generated that way are near optimal, and greatly help the beginning of the CG convergence at a much lower computational cost than exact sub-pricers.

---

#### Algorithm 1 Greedy

---

**Require:** VNE instance

**Ensure:** a mapping for the instance (if one was found)

```

1: Initialize arrays  $m_V[1..n_r] = [0..0]$ 
2:  $m_V[\text{random}(1..n_r)] = \text{random}(1..n_s)$ 
3: for  $i$  in  $1 : n_r - 1$  do
4:    $\bar{u} \leftarrow \text{random}(\bar{v} : m_V(\bar{v}) = 0 :$ 
5:      $|\bar{w} \in N(\bar{v}) : m_V(\bar{w}) \neq 0| \geq 1)$ 
6:    $l_u = \sum_{\bar{v} \in N(\bar{u})} \text{ShortestPath}(m_V(\bar{v}), u)$ 
7:    $m_V[\bar{u}] = \text{argmin}(l_u)$ 
8: end for
9:  $m_E = \text{SuccessiveShortestPathRouting}(m_V)$ 
10: return  $m = (m_V, m_E)$ 

```

---

## 4.5 Lower bounds results

In what follows, we study the performance of our column generation procedure. Our implementation is developed in Julia [58], with Graphs.jl [59] and JuMP [60]. We use the state-of-the-art solver IBM ILOG CPLEX 22.1. In preliminary tests, we tried other solvers such as Gurobi, but CPLEX was the best performing one. All computational experiments were conducted on a machine equipped with an Intel<sup>®</sup> Xeon<sup>®</sup> E5-2650 v3 CPU running at 2.30 GHz.

All the bounds were computed within one hour. Our algorithm is the following. First, 800 columns are generated through the greedy sub-pricers, which, on our setup, takes less than a minute. Then, exact sub-pricers are run for 20 minutes, or until 2500 columns have been generated. Finally, exact pricers are run, which permits the generation of lower Lagrangian bounds. In the tables, the value reported is this Lagrangian bound  $LGB$ .

First, we aim to assess the right partition size, i.e., the number of virtual subgraphs  $k_r$ . Experiments were run on the 10 virtual networks using CogentCo as the substrate network, with large capacities. The Lagrangian lower bounds obtained are reported in Table 2. We also report the average gap to the value of the  $(\widetilde{RMP})$ , which provides a valuable indication of how far column generation is from convergence, and therefore, of the potential for further improvement of the lower bound  $LGB$ . In most instances, the algorithm still presents an important gap (more than 10%) after one hour. The gaps are higher when the substrate network has large capacities and when the virtual networks are larger, which is expected since these instances have more feasible columns. Gaps are also higher for smaller  $k_r$ , i.e., larger virtual subgraphs, for which the sub-pricers become increasingly more difficult. However, smaller  $k_r$  typically lead to better

$k_r$	$\lfloor \frac{n_r}{10} \rfloor + 2$		$\lfloor \frac{n_r}{10} \rfloor + 1$		$\lfloor \frac{n_r}{10} \rfloor$		$\lfloor \frac{n_r}{10} \rfloor - 1$		$\lfloor \frac{n_r}{10} \rfloor - 2$	
	Large	Small	Large	Small	Large	Small	Large	Small	Large	Small
<b>Capacities</b>										
IRIS	180.6	207.0	180.8	206.4	181.7	212.4	183.5	214.8	184.1	211.1
zib54	217.2	260.2	216.8	256.2	212.5	260.6	213.5	237.8	0.0	224.3
Hibernia	222.4	261.4	229.3	270.5	223.5	267.1	210.3	238.8	0.0	0.0
US	225.2	256.3	227.2	259.4	230.8	273.0	213.4	252.9	202.9	254.8
ta2	273.3	329.0	282.0	345.9	276.8	355.0	269.5	328.9	0.0	0.0
TW	297.4	371.8	293.3	367.1	286.4	381.4	287.2	382.7	266.5	358.7
Intellifiber	271.4	311.4	275.1	321.0	285.3	331.0	262.7	312.1	256.0	301.0
Uninett	289.1	333.9	287.2	344.4	268.6	321.4	274.2	337.8	270.4	325.5
OTEGlobe	306.3	352.3	312.5	366.6	308.0	359.6	308.1	371.4	303.8	344.5
Interroute	433.8	502.8	433.7	524.0	437.9	529.3	440.4	536.4	409.4	524.0
<b>Average</b>	271.7	318.6	273.8	326.2	271.2	329.1	266.3	321.4	189.3	254.4
<b>Average gap to v(RMP)</b>	0.14	0.10	0.15	0.11	0.20	0.12	0.29	0.23	-	-

Table 2: Lower bound value and gap to the RMP value, depending on  $k_r$ .

Capacities		Large		Medium		Small	
Algorithm		CG-LB	CPLEX	CG-LB	CPLEX	CG-LB	CPLEX
IRIS	TATA	<b>195</b>	169	<b>191</b>	162	<b>223</b>	197
	GTS	<b>193</b>	176	<b>194</b>	177	<b>220</b>	196
	Cogent	<b>182</b>	170	<b>183</b>	170	<b>213</b>	189
zib54	TATA	<b>225</b>	193	<b>225</b>	188	<b>280</b>	264
	GTS	<b>220</b>	195	<b>231</b>	199	<b>266</b>	239
	Cogent	<b>213</b>	186	<b>217</b>	184	<b>261</b>	216
Hibernia	TATA	<b>235</b>	187	<b>233</b>	188	<b>280</b>	222
	GTS	<b>230</b>	198	<b>230</b>	199	<b>282</b>	216
	Cogent	<b>224</b>	187	<b>225</b>	186	<b>268</b>	210
US	TATA	<b>243</b>	212	<b>242</b>	213	<b>288</b>	250
	GTS	<b>248</b>	214	<b>244</b>	211	<b>285</b>	246
	Cogent	<b>231</b>	200	<b>231</b>	199	<b>273</b>	226
ta2	TATA	<b>299</b>	245	<b>311</b>	251	<b>384</b>	307
	GTS	<b>304</b>	256	<b>311</b>	260	<b>377</b>	299
	Cogent	<b>277</b>	238	<b>278</b>	242	<b>356</b>	279
TW	TATA	<b>311</b>	268	<b>323</b>	278	<b>415</b>	365
	GTS	<b>327</b>	280	<b>336</b>	293	405	<b>418</b>
	Cogent	<b>287</b>	259	<b>300</b>	265	<b>382</b>	347
Intellifiber	TATA	<b>299</b>	254	<b>299</b>	258	<b>359</b>	308
	GTS	<b>303</b>	264	<b>306</b>	264	<b>353</b>	294
	Cogent	<b>286</b>	245	<b>282</b>	245	<b>331</b>	279
Uninett	TATA	<b>292</b>	262	<b>293</b>	262	<b>360</b>	322
	GTS	<b>298</b>	273	<b>297</b>	274	<b>346</b>	307
	Cogent	<b>269</b>	253	<b>269</b>	253	<b>322</b>	288
OTEGlobe	TATA	<b>330</b>	292	<b>327</b>	291	<b>395</b>	353
	GTS	<b>335</b>	298	<b>334</b>	299	<b>396</b>	347
	Cogent	<b>308</b>	276	<b>305</b>	278	<b>360</b>	314
Interroute	TATA	<b>492</b>	448	<b>490</b>	449	<b>607</b>	568
	GTS	<b>501</b>	455	<b>497</b>	456	Inf	<b>Inf</b>
	Cogent	<b>438</b>	406	<b>439</b>	408	<b>530</b>	476
Average	<b>286.1</b>	251.5	<b>287.7</b>	252.9	<b>338.0</b>	293.9	
# best	<b>30</b>	0	<b>30</b>	0	<b>28</b>	2	

Table 3: Lower Bounds obtained on all instances

final values, as discussed in Section 3.3. Hence, the choice of  $k_r$  permits a tradeoff between solving time and bound quality. In the results of our experiments, the best bound values are obtained for  $k_r = \lfloor \frac{n_r}{10} \rfloor$  and  $k_r = \lfloor \frac{n_r}{10} \rfloor + 1$ .

Next, Table 3 shows the results of experiments over all instances. We report the Lagrangian bound we could produce after one hour with  $k_r = \lfloor \frac{n_r}{10} \rfloor$ , and compare it to the bound found by CPLEX after one hour. They show that our column generation consistently finds clearly better lower bounds than CPLEX, beating it on 88 of the 90 instances. Our method allows an average improvement over CPLEX of 13.9% for large capacities, 13.8% for medium capacities, and 11.9% for small capacities. On small capacities, CPLEX performs slightly better. We attribute this to the fact that there are fewer  $x$  variables to branch on, hence the branch-and-bound tree is further advanced after one hour. Overall, these results show that the new Virtual Partition Formulation is much stronger than the Flow Formulation.

**Remark 2.** *The lower bounds of an instance are very close for both large and medium capacity settings, for both our method and CPLEX. This is despite the integer problem being sensibly more difficult, as shown in the next section. To understand this, we observed the fractional solutions, and observed that they spread over most parts of the substrate network. This allows those fractional solutions to keep a low utilization on most substrate edges, which will be only slightly affected by the medium capacity settings. On the other hand, small capacities present sensibly higher bounds, as both edge and node capacities are much more restrictive.*

## 5 Price-and-Branch heuristic

In this section, we will aim to find solutions for the large instances described in Section 2. Greedy heuristics, such as Algorithm 1 or those of [21, 22, 23], perform less well as the virtual network grows. We will show that the Virtual Partition Formulation can be used to find high-quality solutions for the instances considered in this paper. A straightforward approach consists in solving  $(RMP)$  with integer variables after the column generation phase. This is known as a *Price-and-Branch heuristic* (or Restricted Master Problem heuristic). In many decomposition schemes, the columns generated are already well suited for integer solutions, and this heuristic performs well [61]. However, in our case, this algorithm, with columns generated as in Section 4, yielded high costs solutions, or no solutions at all. We identified two issues in the columns produced using the procedure in Section 4. We propose algorithmic improvements to correct these issues. They significantly help integer performance, as shown by the experimental studies.

### 5.1 Intersecting columns

We say that two columns *intersect* when they share at least one substrate node for hosting virtual nodes. In that case, they can not be used together in an integer solution due to the node capacity constraints, although they can be used together in a linear solution of  $(RMP)$  with fractional values. One issue we identified in the previously generated columns is that many of them intersected at the central nodes of the substrate network. To illustrate this, consider Example 2

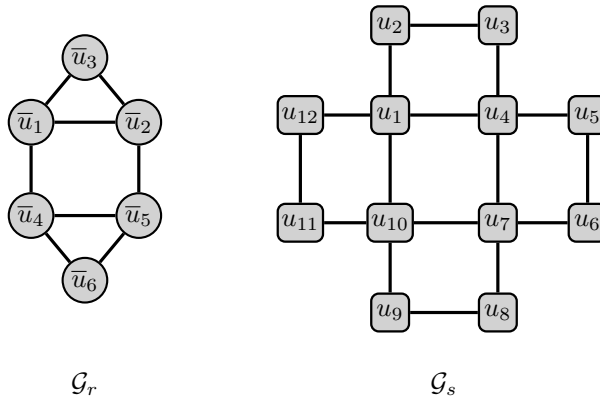


Figure 3: A VNE instance

**Example 2.** *Figure 3 provides an instance of VNE. The virtual network (on the left) is two connected triangles, and has unit demands on every node and edge. The substrate network (on the right) is four connected squares, and has unit capacities on every node and edge, a null cost on every node, and a unit cost on every edge.*

Take the partition  $\pi = (\{\bar{u}_1, \bar{u}_2, \bar{u}_3\}, \{\bar{u}_4, \bar{u}_5, \bar{u}_6\})$  for this virtual network, which gives the two virtual subgraph  $\mathcal{H}_r^1$  and  $\mathcal{H}_r^2$ . Consider the following two sub-mappings for  $\mathcal{H}_r^1$ :

$$\begin{aligned}
m^a : \quad & m_V^a(\bar{u}_1) = u_1, \quad m_V^a(\bar{u}_2) = u_4, \quad m_V^a(\bar{u}_3) = u_2, \\
& m_E^a(\bar{u}_1, \bar{u}_2) = (u_1, u_4) \\
& m_E^a(\bar{u}_2, \bar{u}_3) = (u_4, u_3, u_2), \\
& m_E^a(\bar{u}_3, \bar{u}_1) = (u_2, u_1) \\
m^b : \quad & m_V^b(\bar{u}_1) = u_7, \quad m_V^b(\bar{u}_2) = u_{10}, \quad m_V^b(\bar{u}_3) = u_8, \\
& m_E^b(\bar{u}_1, \bar{u}_2) = (u_7, u_{10}), \\
& m_E^b(\bar{u}_1, \bar{u}_2) = (u_{10}, u_9, u_8), \\
& m_E^b(\bar{u}_3, \bar{u}_1) = (u_8, u_7)
\end{aligned}$$

And, similarly, the two sub-mappings for  $\mathcal{H}_r^2$ :

$$\begin{aligned}
m^c : \quad & m_V^c(\bar{u}_4) = u_4, \quad m_V^c(\bar{u}_5) = u_7, \quad m_V^c(\bar{u}_6) = u_5, \\
& m_E^c(\bar{u}_4, \bar{u}_5) = (u_4, u_7) \\
& m_E^c(\bar{u}_5, \bar{u}_6) = (u_4, u_6, u_5) \\
& m_E^c(\bar{u}_6, \bar{u}_4) = (u_5, u_4) \\
m^d : \quad & m_V^d(\bar{u}_4) = u_{10}, \quad m_V^d(\bar{u}_5) = u_1, \quad m_V^d(\bar{u}_6) = u_{11}, \\
& m_E^d(\bar{u}_4, \bar{u}_5) = (u_{10}, u_1) \\
& m_E^d(\bar{u}_5, \bar{u}_6) = (u_1, u_{12}, u_{11}) \\
& m_E^d(\bar{u}_6, \bar{u}_4) = (u_{11}, u_{10})
\end{aligned}$$

The columns associated all have a cost of 4. With these four columns,  $v(\widetilde{RMP}) = 10$ , with the solution:

$$\begin{aligned}
\lambda_{m_{11}}^1 &= \lambda_{m_{12}}^1 = 0.5, \\
\lambda_{m_{21}}^2 &= \lambda_{m_{22}}^2 = 0.5, \\
y_{(\bar{u}_1, \bar{u}_4)(u_1, u_{10})} &= y_{(\bar{u}_1, \bar{u}_4)(u_7, u_4)} = 0.5, \\
y_{(\bar{u}_2, \bar{u}_5)(u_4, u_1)} &= y_{(\bar{u}_2, \bar{u}_5)(u_{10}, u_4)} = 0.5
\end{aligned}$$

and the other  $y$  variables are set to zero. Here,  $v(\widetilde{RMP}) = v(\widetilde{VPF}_\pi) = v^*$ . However, no integer solutions can be constructed from these columns, as they intersect on nodes  $u_1, u_4, u_7, u_{10}$ .

In practice, we observed that the same central substrate nodes appeared in many columns, which resulted in poor performances of the Price-and-Branch heuristic. To solve this issue, our key idea is to consider a strict partition of the substrate network as follows. Before the beginning of the column generation, the substrate network is partitioned, and columns are then generated with sub-pricers on these substrate subgraphs. This approach has three advantages:

- Columns generated on a substrate subgraph do not intersect with all columns from other substrate subgraphs.
- Assigning coherent parts of the virtual network to coherent parts of the substrate network will induce low-cost sub-mappings within the substrate network.
- Columns can be quickly generated when the substrate subgraphs are small (similar to Section 4.4).

In our experiments, this method significantly improves the performance of the Price-and-Branch heuristic. In most cases, only a few columns per virtual subgraph are sufficient to obtain feasible solutions. Adding more columns further improves solution quality, at the cost of increased computation time. This behavior is mainly due to the integer resolution of the restricted master problem ( $RMP$ ), whose complexity grows exponentially with the number of columns. In practice, solving the ( $RMP$ ) with around 500 columns already often takes more than one minute.

With this implementation, the quality of the obtained solution depends strongly on the partitions computed for both the virtual and substrate networks. To generate these partitions, we also use METIS and KaHIP, as described in Section 4.1. The size of the substrate subgraphs also plays a crucial role in the effectiveness of the heuristic. If the substrate subgraphs are too small, the sub-pricers may become infeasible or produce expensive columns. To illustrate this remark,

consider a virtual and a substrate subgraph of the same number of nodes. When the virtual is denser than the substrate, then long virtual edge routing paths are necessary. Conversely, very large subgraphs produce cheaper columns, but can result in higher routing costs for the cut edges. Based on our preliminary experiments, a good choice is to partition the substrate network into balanced subgraphs whose average size (number of capacitated nodes) is about 1.5 times the maximum size of the virtual subgraphs. This ratio, however, may vary depending on the demand and capacity settings.

## 5.2 Better virtual boundary node placements

In a graph partition, a *boundary node* is a node adjacent to a cut edge, whereas a node with no neighbors outside its subgraph is called an *internal node*. A second issue we observed in the generated columns is that the virtual boundary nodes are often placed on internal substrate nodes. This induces longer routing paths for virtual cut edge. To illustrate this, consider again the instance of Example 2. Take the partition  $\pi = (\{\bar{u}_1, \bar{u}_2, \bar{u}_3\}, \{\bar{u}_4, \bar{u}_5, \bar{u}_6\})$ . Here, the virtual boundary nodes  $\bar{u}_1, \bar{u}_2, \bar{u}_4, \bar{u}_5$  have to be placed on the substrate boundary nodes  $u_1, u_4, u_7, u_{10}$ , otherwise no solution exists. However, throughout our experiments, we observed that virtual boundary nodes were often placed on outlier substrate nodes.

To tackle poor boundary placements, our key idea is to modify the objective functions of the sub-pricers to incorporate an estimation of routing costs for virtual cut edges. This is done through Algorithm 2, which, given the virtual and substrate partitions, generates  $k_r$  columns (one per virtual subgraph) as follows. Each virtual subgraph is assigned to a distinct substrate subgraph (array  $a$ ), and virtual nodes have temporary placements (array  $t_V$ ). At the beginning, this temporary placement corresponds to the most central substrate node of the substrate subgraph to which they are assigned to (function `Center`). To do this, we use closeness centrality defined in [62]. When embedding a subgraph, the cost of placing a boundary node is adjusted by the shortest-path distance (function `ShortestPath`) to the temporary placements of its neighbors in other substrate subgraphs. To this end, we use the Floyd-Warshall algorithm described in [63]. This adjustment makes substrate boundary nodes more attractive for virtual boundary nodes, and generated columns (function `SolveSubPricer`) are more consistent with each other as they take into account the sub-mapping of other subgraphs. The assignment of virtual subgraph to substrate subgraph is randomly decided.

---

### Algorithm 2 GenerateIntegerColumns

---

**Require:** VNE instance, dual variables, Virtual partition  $\pi_r$ , substrate partition  $\pi_s$

**Ensure:**  $k_r$  sub-mappings (one per virtual subgraph)

```

1: Initialize arrays  $a[1..k_r]$ ,  $t_V[1..n_r]$ 
2: for  $\mathcal{H}_r^i \in \pi_r$  do
3:    $a[i] \leftarrow \mathcal{H}_s^j \in \pi_s \setminus a$ 
4:    $u_c \leftarrow \text{Center}(a[i])$ 
5:    $t_V[\bar{u}] \leftarrow u_c \quad \forall \bar{u} \in V(\mathcal{H}_r^i)$ 
6: end for
7: for  $\mathcal{H}_r^i \in \pi_r$  do
8:    $w_{\bar{u}u} \leftarrow w_u \quad \forall \bar{u} \in V_r, u \in V_s$ 
9:   for  $\bar{e} \in E_r^0$  with  $t(\bar{e}) \in V_r^i$  do
10:     $\hat{w}_u^{t(\bar{e})} \leftarrow w_u + \text{ShortestPath}(t_V(s(\bar{e})), u)$ 
11:   end for
12:   for  $\bar{e} \in E_r^0$  with  $s(\bar{e}) \in V_r^i$  do
13:     $\hat{w}_u^{s(\bar{e})} \leftarrow w_u + \text{ShortestPath}(t_V(t(\bar{e})), u)$ 
14:   end for
15:    $m^i \leftarrow \text{SolveSubPricer}(\mathcal{H}_r^i, a[i], \hat{w}, \text{dual vars})$ 
16:    $t_V[\bar{u}] \leftarrow m_V^i(\bar{u}) \quad \forall \bar{u} \in V_r^i$ 
17: end for
18: return  $\{m^i : \mathcal{H}_r^i \in \pi_r\}$ 

```

---

In our Price-and-Branch heuristic, Algorithm 2 is used until a given number of columns is generated. Preliminary experiments showed that incorporating routing-cost estimations improves solution quality by 5–10%, with no increase in solving time.

## 5.3 Heuristics results

We first tune the parameters  $k_r$  and the number of used columns using instances with large capacities. Then we run tests over the whole instance set using the chosen parameters.

Pricer	Greedy					CPLEX				
	$\lfloor \frac{n_r}{10} \rfloor + 2$	$\lfloor \frac{n_r}{10} \rfloor + 1$	$\lfloor \frac{n_r}{10} \rfloor$	$\lfloor \frac{n_r}{10} \rfloor - 1$	$\lfloor \frac{n_r}{10} \rfloor - 2$	$\lfloor \frac{n_r}{10} \rfloor + 2$	$\lfloor \frac{n_r}{10} \rfloor + 1$	$\lfloor \frac{n_r}{10} \rfloor$	$\lfloor \frac{n_r}{10} \rfloor - 1$	$\lfloor \frac{n_r}{10} \rfloor - 2$
$k_r$										
IRIS	293	308	299	289	282	292	293	290	274	267
zib54	373	399	402	386	355	364	390	380	345	335
Hibernia	358	372	366	379	353	350	357	333	333	320
US	386	383	385	382	384	376	366	363	360	355
ta2	530	553	548	544	550	536	527	528	510	485
TW	563	593	619	622	629	581	592	587	555	576
Intellifiber	470	476	461	451	458	445	445	433	443	418
Uninett	515	519	573	531	531	491	506	546	512	491
OTEGlobe	510	501	520	502	479	489	478	488	471	444
Interroute	844	818	793	809	780	801	800	771	762	745
<b>Average cost</b>	484.2	492.2	496.6	489.5	480.1	472.5	475.4	471.9	456.5	443.6
<b>Time (s)</b>	18.0	24.5	20.8	19.5	20.3	62.7	72.6	89.7	256.5	1970.8

Table 4: Price-and-Branch heuristic performance depending on the number of virtual subgraphs

Pricer	Greedy						CPLEX					
	$k_r$	25	50	100	200	500	$k_r$	25	50	100	200	500
IRIS	373	344	335	317	299	300	407	321	302	296	290	287
zib54	556	430	420	411	402	394	526	405	396	384	380	369
Hibernia	520	411	386	373	366	349	472	380	362	344	333	324
US	524	437	417	382	385	374	477	397	377	371	363	356
ta2	867	618	621	563	548	553	691	584	553	539	528	515
TW	852	684	669	640	619	609	817	659	614	605	587	564
Intellifiber	654	492	477	474	461	442	562	485	456	440	433	419
Uninett	845	629	622	599	573	554	755	612	585	560	546	530
OTEGlobe	737	565	544	527	520	505	602	532	512	496	488	476
Interroute	911	899	908	812	793	760	928	857	809	793	771	734
<b>Average cost</b>	683.9	550.9	539.9	509.8	496.6	484.0	623.7	523.2	496.6	482.8	471.9	457.4
<b>Time (s)</b>	0.9	1.9	3.3	5.5	20.8	237.1	2.9	10.9	20.0	41.6	89.7	360.1

Table 5: Price-and-Branch heuristic performance depending on the number of columns

First, we study the influence of the partition size  $k_r$  on the Price-and-Branch heuristic, with 200 columns generated by greedy or exact (CPLEX) pricers, with Algorithm 2. The results are reported in Table 4. With greedy pricers, solving times and solution quality remain quite stable. Greedy sub-pricers are quite competitive for high  $k_r$ , since near-optimal solutions can be found with small virtual subgraphs,. On the other hand, for exact pricers, we find better solutions with  $k_r \geq \lfloor \frac{n_r}{10} \rfloor$ . The best solutions are found with  $k_r = \lfloor \frac{n_r}{10} \rfloor - 2$ , with, unfortunately, very long solving times, as the sub-pricers become more difficult. From now on we opt for  $k_r = \lfloor \frac{n_r}{10} \rfloor$ .

Next, we study the impact of the number of columns. The results are reported in Table 5. As expected, using more columns leads to better solutions. Since the solving time of the integer Restricted Master Problem increases exponentially, we used a time limit of 600 seconds, which was often met with 500 columns. Again, using exact pricers, compared to greedy algorithms, improves the performance on average by 5 to 10%, at the cost of higher solving times. From now on, we opt for 200 columns and solving sub-pricers with CPLEX.

Finally, we evaluate our Price-and-Branch heuristic on the full set of instances. On average, the heuristic runs for about 100 seconds. We compare our approach with two alternatives:

- (1) the greedy heuristic Algorithm 1, executed repeatedly for 100 seconds, leading to several thousand iterations, among which we keep the best one.
- (2) CPLEX in heuristic mode, with a time limit of 100 seconds. The results are summarized in Table 6. When an algorithm fails to produce a solution, the corresponding cell is marked “-”. We can see that our heuristic consistently outperforms the baselines on all solved instances.

With large capacities, every node placement leads to a feasible solution. CPLEX already struggles to find solutions due to the very large size of the model, whereas our heuristic and the greedy algorithm always find a solution. The embeddings found by our heuristic are significantly better. When capacities are tighter, the advantage of our method becomes more pronounced: both greedy heuristics and CPLEX find solutions only in about half of the instances with medium capacities, and almost none with small capacities. This is expected for the greedy heuristic, which relies on progressive node placement and a successive shortest path algorithm for edge routing. Meanwhile, our algorithm is still able to find solutions for most instances with medium capacities. On small-capacity instances, our heuristic finds fewer feasible solutions, particularly for large and dense virtual networks, which are naturally more challenging as they induce much more (cut) edge routing, but still largely outperforms the other algorithms.

Capacities		Large			Medium			Small		
Algorithm		PBH	Greedy	CPLEX	PBH	Greedy	CPLEX	PBH	Greedy	CPLEX
IRIS	TATA	<b>310</b>	352	366	319	400	460	413	-	-
	GTS	<b>316</b>	363	470	308	360	464	370	483	-
	Cogent	<b>292</b>	342	619	287	339	521	335	422	478
zib54	TATA	<b>409</b>	527	759	424	-	-	-	-	-
	GTS	<b>390</b>	487	1011	401	678	573	-	-	-
	Cogent	<b>377</b>	485	707	434	-	742	-	-	-
Hibernia	TATA	<b>368</b>	513	662	365	571	685	457	-	-
	GTS	<b>348</b>	476	620	364	540	-	441	-	525
	Cogent	<b>339</b>	489	725	344	663	697	411	-	-
US	TATA	<b>372</b>	507	735	374	514	738	470	-	608
	GTS	<b>366</b>	471	565	371	469	753	439	-	-
	Cogent	<b>365</b>	467	840	359	474	582	398	-	-
ta2	TATA	<b>576</b>	752	1578	710	-	-	-	-	-
	GTS	<b>546</b>	699	1723	597	-	-	-	-	-
	Cogent	<b>537</b>	700	-	-	-	-	-	-	-
TW	TATA	<b>647</b>	797	-	849	-	-	-	-	-
	GTS	<b>641</b>	728	-	-	-	-	-	-	-
	Cogent	<b>574</b>	739	-	-	-	-	-	-	-
Intellifiber	TATA	<b>452</b>	630	1088	453	706	838	596	-	-
	GTS	<b>445</b>	585	1247	460	653	829	549	-	-
	Cogent	<b>425</b>	584	864	450	661	847	511	-	-
Uninett	TATA	<b>620</b>	693	1312	794	-	-	-	-	-
	GTS	<b>590</b>	635	1330	-	-	-	-	-	-
	Cogent	<b>551</b>	632	-	659	-	-	-	-	-
OTEGlobe	TATA	<b>528</b>	649	1437	535	722	742	684	-	-
	GTS	<b>522</b>	631	1211	501	693	833	-	-	-
	Cogent	<b>485</b>	647	-	483	770	876	564	-	-
Interoute	TATA	<b>824</b>	1048	-	860	-	-	-	-	-
	GTS	<b>821</b>	1032	-	834	-	-	-	-	Inf
	Cogent	<b>761</b>	1015	-	788	-	-	-	-	-
# feasible		<b>30</b>	<b>30</b>	22	<b>26</b>	16	16	<b>14</b>	2	3
# best		<b>30</b>	0	0	<b>26</b>	0	0	<b>14</b>	0	1

Table 6: Price-Branch Heuristic results

## 6 Conclusion

This paper introduces a new integer linear programming formulation for Virtual Network Embedding, based on a partition of the virtual network. We propose an automatic decomposition scheme that allows a good trade-off between the size of the partition and the efficiency of the pricing problems. A first column generation approach using dedicated heuristic pricers is able to compute better lower bounds than state-of-the-art methods. In the aim of producing solutions, we identified some column structures and devised a Price-and-Branch heuristic that obtains solutions for instances with large virtual networks, up to 110 nodes in our tests. This heuristic outperforms the algorithms from the literature for large instances of the Internet Topology Zoo and SNDlib, in particular with tight capacities instances, while greedy approaches fail to solve them.

Within the instance benchmark we have compiled from the literature, some instances are still unsolved. Leveraging the decomposition technique using other partition schemes where the virtual subgraphs can overlap should produce better lower bounds. Since the pricers are based on the Flow Formulation, a reinforcement through valid inequalities based on a polyhedral study, will allow improvements in the efficiency of our method. Finally, to improve the initial solution we proposed, local search methods should be investigated to reduce the gap between the lower and upper bounds we produced.

## References

- [1] Thomas Anderson, Larry Peterson, Scott Shenker, and Jonathan Turner. Overcoming the internet impasse through virtualization. *Computer*, 38(4):34–41, 2005.

- [2] Jonathan S Turner and David E Taylor. Diversifying the internet. In *GLOBECOM'05. IEEE Global Telecommunications Conference, 2005.*, volume 2, pages 6–pp. IEEE, 2005.
- [3] NM Mosharaf Kabir Chowdhury and Raouf Boutaba. A survey of network virtualization. *Computer Networks*, 54(5):862–876, 2010.
- [4] NGMN Alliance. Description of network slicing concept. *NGMN 5G P*, 1(1):1–11, 2016.
- [5] 3rd Generation Partnership Project. 5g; management and orchestration; concepts, use cases and requirements, release 15, ts 28.530. 2018.
- [6] Xenofon Foukas, Georgios Patounas, Ahmed Elmokashfi, and Mahesh K Marina. Network slicing in 5g: Survey and challenges. *IEEE communications magazine*, 55(5):94–100, 2017.
- [7] Jose Ordonez-Lucena, Pablo Ameigeiras, Diego Lopez, Juan J Ramos-Munoz, Javier Lorca, and Jesus Folgueira. Network slicing for 5g with sdn/nfv: Concepts, architectures, and challenges. *IEEE Communications Magazine*, 55(5):80–87, 2017.
- [8] Ibrahim Afolabi, Tarik Taleb, Konstantinos Samdanis, Adlen Ksentini, and Hannu Flinck. Network slicing and softwarization: A survey on principles, enabling technologies, and solutions. *IEEE Communications Surveys & Tutorials*, 20(3):2429–2453, 2018.
- [9] T-Mobile. America’s best 5g network experience for first responders, 2025.
- [10] Siemens. Siemens and o2 telefónica partner to develop solutions based on 5g network slicing, 2025.
- [11] Jing Lu and Jonathan Turner. Efficient mapping of virtual networks onto a shared substrate. 2006.
- [12] Y. Zhu and M. Ammar. Algorithms for assigning substrate network resources to virtual network components. In *Proceedings IEEE INFOCOM 2006. 25TH IEEE International Conference on Computer Communications*, pages 1–12, 2006.
- [13] Spyridon Vassilaras, Lazaros Gkatzikis, Nikolaos Liakopoulos, Ioannis N Stiakogiannakis, Meiyu Qi, Lei Shi, Liu Liu, Merouane Debbah, and Georgios S Paschos. The algorithmic aspects of network slicing. *IEEE Communications Magazine*, 55(8):112–119, 2017.
- [14] Edoardo Amaldi, Stefano Coniglio, Arie MCA Koster, and Martin Tieves. On the computational complexity of the virtual network embedding problem. *Electronic Notes in Discrete Mathematics*, 52:213–220, 2016.
- [15] Matthias Rost and Stefan Schmid. On the hardness and inapproximability of virtual network embeddings. *IEEE/ACM transactions on networking*, 28(2):791–803, 2020.
- [16] Amal Benhamiche, Pierre Fouilhoux, Lucas Létocart, Nancy Perrot, and Alexis Schneider. Complexity of the virtual network embedding with uniform demands. *arXiv preprint arXiv:2501.10154*, 2025.
- [17] Matthias Rost, Carlo Fuerst, and Stefan Schmid. Beyond the stars: Revisiting virtual cluster embeddings. *ACM SIGCOMM Computer Communication Review*, 45(3):12–18, 2015.
- [18] Andreas Fischer, Juan Felipe Botero, Michael Till Beck, Hermann De Meer, and Xavier Hesselbach. Virtual network embedding: A survey. *IEEE Communications Surveys & Tutorials*, 15(4):1888–1906, 2013.
- [19] Mosharaf Chowdhury, Muntasir Raihan Rahman, and Raouf Boutaba. Vineyard: Virtual network embedding algorithms with coordinated node and link mapping. *IEEE/ACM Transactions on networking*, 20(1):206–219, 2011.
- [20] Minlan Yu, Yung Yi, Jennifer Rexford, and Mung Chiang. Rethinking virtual network embedding: Substrate support for path splitting and migration. *ACM SIGCOMM Computer Communication Review*, 38(2):17–29, 2008.
- [21] Xiang Cheng, Sen Su, Zhongbao Zhang, Hanchi Wang, Fangchun Yang, Yan Luo, and Jie Wang. Virtual network embedding through topology-aware node ranking. *ACM SIGCOMM Computer Communication Review*, 41(2):38–47, 2011.
- [22] Long Gong, Yonggang Wen, Zuqing Zhu, and Tony Lee. Toward profit-seeking virtual network embedding algorithm via global resource capacity. In *IEEE INFOCOM 2014-IEEE Conference on Computer Communications*, pages 1–9. IEEE, 2014.
- [23] Peiyong Zhang, Haipeng Yao, and Yunjie Liu. Virtual network embedding based on the degree and clustering coefficient information. *IEEE Access*, 4:8572–8580, 2016.
- [24] Johannes Inführ and Günther R Raidl. Solving the virtual network mapping problem with construction heuristics, local search and variable neighborhood descent. In *European Conference on Evolutionary Computation in Combinatorial Optimization*, pages 250–261. Springer, 2013.

- [25] Amine Rguez, Yassine Hadjadj-Aoul, and Gerardo Rubino. A grasp-based approach for dynamic and reliable virtual network embedding. In *2025 Global Information Infrastructure and Networking Symposium (GIIS)*, pages 1–6. IEEE, 2025.
- [26] Zhongbao Zhang, Xiang Cheng, Sen Su, Yiwen Wang, Kai Shuang, and Yan Luo. A unified enhanced particle swarm optimization-based virtual network embedding algorithm. *International Journal of Communication Systems*, 26(8):1054–1073, 2013.
- [27] Peiyong Zhang, Yanrong Hong, Xue Pang, and Chunxiao Jiang. Vne-hpso: Virtual network embedding algorithm based on hybrid particle swarm optimization. *IEEE Access*, 8:213389–213400, 2020.
- [28] Ilhem Fajjari, Nadjib Aitsaadi, Guy Pujolle, and Hubert Zimmermann. Vne-ac: Virtual network embedding algorithm based on ant colony metaheuristic. In *2011 IEEE international conference on communications (ICC)*, pages 1–6. IEEE, 2011.
- [29] Peiyong Zhang, Haipeng Yao, Maozhen Li, and Yunjie Liu. Virtual network embedding based on modified genetic algorithm. *Peer-to-Peer Networking and Applications*, 12(2):481–492, 2019.
- [30] Xu Liu, Zhongbao Zhang, Ximing Li, and Sen Su. Optimal virtual network embedding based on artificial bee colony. *EURASIP Journal on Wireless Communications and Networking*, 2016(1):273, 2016.
- [31] Fangjin Zhu and Hua Wang. A modified aco algorithm for virtual network embedding based on graph decomposition. *Computer Communications*, 80:1–15, 2016.
- [32] An Song, Wei-Neng Chen, Yue-Jiao Gong, Xiaonan Luo, and Jun Zhang. A divide-and-conquer evolutionary algorithm for large-scale virtual network embedding. *IEEE Transactions on Evolutionary Computation*, 24(3):566–580, 2019.
- [33] Soroush Haeri and Ljiljana Trajković. Virtual network embedding via monte carlo tree search. *IEEE transactions on cybernetics*, 48(2):510–521, 2017.
- [34] Haipeng Yao, Xu Chen, Maozhen Li, Peiyong Zhang, and Luyao Wang. A novel reinforcement learning algorithm for virtual network embedding. *Neurocomputing*, 284:1–9, 2018.
- [35] Mahdi Dolati, Seyedeh Bahereh Hassanpour, Majid Ghaderi, and Ahmad Khonsari. Deepvine: Virtual network embedding with deep reinforcement learning. In *IEEE INFOCOM 2019-IEEE Conference on Computer Communications Workshops (INFOCOM WKSHPS)*, pages 879–885. IEEE, 2019.
- [36] Farzad Habibi, Mahdi Dolati, Ahmad Khonsari, and Majid Ghaderi. Accelerating virtual network embedding with graph neural networks. In *2020 16th International Conference on Network and Service Management (CNSM)*, pages 1–9. IEEE, 2020.
- [37] Zhongxia Yan, Jingguo Ge, Yulei Wu, Liangxiong Li, and Tong Li. Automatic virtual network embedding: A deep reinforcement learning approach with graph convolutional networks. *IEEE Journal on Selected Areas in Communications*, 38(6):1040–1057, 2020.
- [38] NM Mosharaf Kabir Chowdhury, Muntasir Raihan Rahman, and Raouf Boutaba. Virtual network embedding with coordinated node and link mapping. In *IEEE INFOCOM 2009*, pages 783–791. IEEE, 2009.
- [39] Marcio Melo, Susana Sargento, Ulrich Killat, Andreas Timm-Giel, and Jorge Carapinha. Optimal virtual network embedding: Node-link formulation. *IEEE Transactions on Network and Service Management*, 10(4):356–368, 2013.
- [40] Leonardo FS Moura, Luciano P Gaspary, and Luciana S Buriol. A branch-and-price algorithm for the single-path virtual network embedding problem. *Networks*, 71(3):188–208, 2018.
- [41] Matthias Rost and Stefan Schmid. Virtual network embedding approximations: Leveraging randomized rounding. *IEEE/ACM Transactions on Networking*, 27(5):2071–2084, 2019.
- [42] Rashid Mijumbi, Joan Serrat, Juan-Luis Gorricho, and Raouf Boutaba. A path generation approach to embedding of virtual networks. *IEEE Transactions on Network and Service Management*, 12(3):334–348, 2015.
- [43] Abdallah Jarray and Ahmed Karmouch. Decomposition approaches for virtual network embedding with one-shot node and link mapping. *IEEE/ACM Transactions on Networking*, 23(3):1012–1025, 2014.
- [44] Matthias Rost, Elias Döhne, and Stefan Schmid. Parametrized complexity of virtual network embeddings: Dynamic & linear programming approximations. *ACM SIGCOMM Computer Communication Review*, 49(1):3–10, 2019.
- [45] Peiyong Zhang, Haipeng Yao, and Yunjie Liu. Virtual network embedding based on computing, network, and storage resource constraints. *IEEE Internet of Things Journal*, 5(5):3298–3304, 2017.
- [46] Alexis Schneider. Vne lib: a library for offline virtual network embedding instances, 2021.

- [47] Ellen W Zegura, Kenneth L Calvert, and Samrat Bhattacharjee. How to model an internet network. In *Proceedings of IEEE INFOCOM'96. Conference on Computer Communications*, volume 2, pages 594–602. IEEE, 1996.
- [48] Simon Knight, Hung X Nguyen, Nickolas Falkner, Rhys Bowden, and Matthew Roughan. The internet topology zoo. *IEEE Journal on Selected Areas in Communications*, 29(9):1765–1775, 2011.
- [49] Sebastian Orłowski, Roland Wessälly, Michal Pióro, and Artur Tomaszewski. Sndlib 1.0—survivable network design library. *Networks: An International Journal*, 55(3):276–286, 2010.
- [50] Wesley da Silva Coelho, Amal Benhamiche, Nancy Perrot, and Stefano Secci. On the impact of novel function mappings, sharing policies, and split settings in network slice design. In *2020 16th international conference on network and service management (CNSM)*, pages 1–9. IEEE, 2020.
- [51] Ravindra K Ahuja, Thomas L Magnanti, and James B Orlin. *Network flows*. 1988.
- [52] Christian Raack, Arie MCA Koster, Sebastian Orłowski, and Roland Wessälly. On cut-based inequalities for capacitated network design polyhedra. *Networks*, 57(2):141–156, 2011.
- [53] Jacques Desrosiers and Marco E Lübbecke. A primer in column generation. In Springer, editor, *Column generation*, pages 1–32. Springer, 2005.
- [54] Alberto Caprara, Fabio Furini, Enrico Malaguti, and Emiliano Traversi. Solving the temporal knapsack problem via recursive dantzig–wolfe reformulation. *Information Processing Letters*, 116(5):379–386, 2016.
- [55] Peter Sanders and Christian Schulz. Think locally, act globally: Highly balanced graph partitioning. In *International Symposium on Experimental Algorithms*, pages 164–175. Springer, 2013.
- [56] George Karypis and Vipin Kumar. Metis: A software package for partitioning unstructured graphs, partitioning meshes, and computing fill-reducing orderings of sparse matrices. 1997.
- [57] Artur Pessoa, Ruslan Sadykov, Eduardo Uchoa, and Francois Vanderbeck. In-out separation and column generation stabilization by dual price smoothing. In *International Symposium on Experimental Algorithms*, pages 354–365. Springer, 2013.
- [58] Jeff Bezanson, Alan Edelman, Stefan Karpinski, and Viral B Shah. Julia: A fresh approach to numerical computing. *SIAM review*, 59(1):65–98, 2017.
- [59] James Fairbanks, Mathieu Besançon, Schölly Simon, Júlio Hoffiman, Nick Eubank, and Stefan Karpinski. *Juliagraphs/graphs.jl: an optimized graphs package for the julia programming language*, 2021.
- [60] Iain Dunning, Joey Huchette, and Miles Lubin. Jump: A modeling language for mathematical optimization. *SIAM review*, 59(2):295–320, 2017.
- [61] Ze Wang, Tim Süß, Nikolay Popov, and Lars Nagel. Price-and-branch heuristic for vector bin packing. In Martin S. Krejca and Markus Wagner, editors, *Evolutionary Computation in Combinatorial Optimization*, pages 249–265, Cham, 2025. Springer Nature Switzerland.
- [62] Gert Sabidussi. The centrality index of a graph. *Psychometrika*, 31(4):581–603, 1966.
- [63] Robert W Floyd. Algorithm 97: shortest path. *Communications of the ACM*, 5(6):345–345, 1962.